Organometallics **2001,** *20,* 1752−1761

Synthesis and Olefin Polymerization Catalysis of New Trivalent Samarium and Yttrium Complexes with Bridging Bis(cyclopentadienyl) Ligands

Eiji Ihara,[†] Shiro Yoshioka,[†] Masahito Furo,[†] Kenji Katsura,[†] Hajime Yasuda,*,[†]
Shouhei Mohri,[‡] Nobuko Kanehisa,[‡] and Yasushi Kai*,[‡]

Department of Applied Chemistry, Faculty of Engineering, Hiroshima University,
Higashi-Hiroshima 739-8527, Japan, and Department of Applied Chemistry,
Faculty of Engineering, Osaka University, Suita 565-0871, Japan

Received March 14, 2000

New trivalent samarium and yttrium complexes with bridging bis(cyclopentadienyl) ligands were synthesized, and olefin polymerization catalysis of the complexes having an alkyl group $[\mathrm{R = CH(SiMe_3)_2}]$ on the metal was investigated. Three types of the rare earth halides (*rac*, C_1, and *meso*) whose structures differed with respect to the bridging group and the positions of substituents on the cyclopentadienyl (Cp) rings were prepared: *rac*-Sm−Cl, $\mathrm{Me_2Si[2,4\text{-}(Me_3Si)_2C_5H_2]_2SmCl_2Li(THF)_2}$ (**1a**); C_1-Sm−Cl, $\mathrm{Me_2Si[2,4\text{-}(Me_3Si)_2C_5H_2][3,4\text{-}(Me_3Si)_2C_5H_2]SmCl_2Li(THF)_2}$ (**2a**); $C_1(\mathrm{Ph_2Si})$−Sm−Cl, $\mathrm{Ph_2Si[2,4\text{-}(Me_3Si)_2C_5H_2][3,4\text{-}(Me_3Si)_2C_5H_2]SmCl_2Li(THF)_2}$ (**3**); *meso*-Sm−Cl, $\mathrm{[1,2\text{-}(Me_2Si)(Me_2SiOSiMe_2)](4\text{-}Me_3CC_5H_2)_2SmCl_2Li(THF)_2}$ (**4a**); *rac*-Y−Cl, $\mathrm{Me_2Si[2,4\text{-}(Me_3Si)_2C_5H_2]_2YCl_2Li(THF)_2}$ (**5a**); C_1-Y−Cl, $\mathrm{Me_2Si[2,4\text{-}(Me_3Si)_2C_5H_2][3,4\text{-}(Me_3Si)_2C_5H_2]YCl_2Li(THF)_2}$ (**6a**); *meso*-Y−Cl, $\mathrm{[1,2\text{-}(Me_2Si)(Me_2SiOSiMe_2)](4\text{-}Me_3SiC_5H_2)_2YCl(THF)}$ (**7a**). Although the *rac* and C_1 complexes (**1a**, **2a** and **5a**, **6a**) were obtained as an isomeric mixture by the reaction of $\mathrm{LnCl_3}$ (Ln = Sm, Y) with a dilithium salt of the ligand $\mathrm{Me_2Si[(Me_3Si)_2C_5H_3]_2}$, it could be separated into both the pure complexes by utilizing the difference of solubility in hexane in each case. Structural data were obtained on **1a**, **2a**, **3**, and **7a** to confirm the structures expected from NMR spectroscopy. The (ring centroid)−metal−(ring centroid) angles in these complexes are ca. 10−20° smaller than those in nonbridging bis(cyclopentadienyl) rare earth complexes. The rare earth halides **1a**, **2a**, **4a**, **5a**, **6a**, and **7a** reacted with $\mathrm{LiCH(SiMe_3)_2}$ to afford rare earth alkyl complexes, *rac*-Sm−R, $\mathrm{Me_2Si[2,4\text{-}(Me_3Si)_2C_5H_2]_2SmCH(SiMe_3)_2}$ (**1b**); C_1-Sm−R, $\mathrm{Me_2Si[2,4\text{-}(Me_3Si)_2C_5H_2][3,4\text{-}(Me_3Si)_2C_5H_2]SmCH(SiMe_3)_2}$ (**2b**); *meso*-Sm−R, $\mathrm{[1,2\text{-}(Me_2Si)(Me_2SiOSiMe_2)](4\text{-}Me_3CC_5H_2)_2SmCH(SiMe_3)_2}$ (**4b**); *rac*-Y−R, $\mathrm{Me_2Si[2,4\text{-}(Me_3Si)_2C_5H_2]_2YCH(SiMe_3)_2}$ (**5b**); C_1-Y−R, $\mathrm{Me_2Si[2,4\text{-}(Me_3Si)_2C_5H_2][3,4\text{-}(Me_3Si)_2C_5H_2]YCH(SiMe_3)_2}$ (**6b**); *meso*-Y−R, and $\mathrm{[1,2\text{-}(Me_2Si)(Me_2SiOSiMe_2)](4\text{-}Me_3SiC_5H_2)_2YCH(SiMe_3)_2}$ (**7b**), respectively. Only C_1 type alkyl complexes (**2b** and **6b**) polymerize ethylene, giving high molecular weight polyethylenes, and the precise structure of the active Sm complex **2b** was determined by X-ray crystallography.

Introduction

Since it was found that the trivalent bis(pentamethylcyclopentadienyl) (bis-Cp*) rare earth metal complexes $\mathrm{Cp^*_2LnR}$ possessed ethylene polymerization activity in the early 1980s,[1] much attention has been paid to this class of single-component olefin polymerization catalysts.[2] Mechanistic details of the polymerization were revealed using $\mathrm{Cp^*_2LuR}$[1c,2d] and $\mathrm{Cp^*_2ScR}$.[2k,l] $\mathrm{(Cp^*_2LaH)_2}$ has been shown to have high ethylene polymerization activity comparable to those of Kaminsky type catalysts, although the complex gave low molecular weight oligomers by the reaction with 1-olefins.[2n] It has been shown that the divalent bis-Cp* Sm compound ($\mathrm{Cp^*_2SmL}$) can also act as an initiator.[1a] Detailed mechanistic studies on $\mathrm{Cp^*_2Sm}$- and $[\mathrm{Cp^*_2Sm}(\mu\text{-H})]_2$-initiated olefin polymerization using field desorption mass spectrometry have been reported.[2f,g] Although the inherent air sen-

---

[†] Hiroshima University.

[‡] Osaka University.

(1) (a) Watson, P. L.; Herskovitz, T. *ACS Symp. Ser.* **1983**, *212*, 459−479. (b) Watson, P. L.; Parshall, G. W. *Acc. Chem. Res.* **1985**, *18*, 51−56. (c) Watson, P. L.; Roe, D. C. *J. Am. Chem. Soc.* **1982**, *104*, 6471−6473. (d) Watson, P. L. *J. Am. Chem. Soc.* **1982**, *104*, 337−339.

(2) (a) Yasuda, H.; Ihara, E. *Adv. Polym. Sci.* **1997**, *133*, 53−101. (b) Ihara, E.; Nodono, M.; Katsura, K.; Adachi, Y.; Yasuda, H.; Yamagashira, M.; Hashimoto, H.; Kanehisa, N.; and Kai, Y. *Organometallics* **1998**, *17*, 3945−3956. (c) Long, D. P.; Bianconi, P. A. *J. Am. Chem. Soc.* **1996**, *118*, 12453−12454. (d) Gilchrist, J. H.; Bercaw, J. E. *J. Am. Chem. Soc.* **1996**, *118*, 12021−12028. (e) Mitchell, J. P.; Hajela, S.; Brookhart, S. K.; Hardcastle, K. I.; Henling, L. M.; Bercaw, J. E. *J. Am. Chem. Soc.* **1996**, *118*, 1045−1053. (f) Evans, W. J.; DeCoster, D. M.; Greaves, J. *Organometallics* **1996**, *15*, 3210−3221. (g) Evans, W. J.; DeCoster, D. M.; Greaves, J. *Macromolecules* **1995**, *28*, 7929−7936. (h) Shapiro, P. J.; Cotter, W. D.; Schaefer, W. P.; Labinger, J. A.; Bercaw, J. E. *J. Am. Chem. Soc.* **1994**, *116*, 4623−4640. (i) Schaverien, C. J. *Organometallics* **1994**, *13*, 69−82. (j) Coughlin, E. B. *J. Am. Chem. Soc.* **1992**, *114*, 7606−7607. (k) Piers, W. E.; Bercaw, J. E. *J. Am. Chem. Soc.* **1990**, *112*, 9406−9407. (l) Burger, B. J.; Thompson, M. E., Cotter, W. D.; Bercaw, J. E. *J. Am. Chem. Soc.* **1990**, *112*, 1566−1577. (m) Shapiro, P. J.; Bunel, E.; Schaefer, W. P. *Organometallics* **1990**, *9*, 867−869. (n) Jeske, G.; Lauke, H.; Mauermann, H.; Swepston, P. N.; Schumann, H.; Marks, T. J. *J. Am. Chem. Soc.* **1985**, *107*, 8091−8103. (o) Jeske, G.; Schock, L. E.; Swepston, P. N.; Schumann, H.; Marks, T. J. *J. Am. Chem. Soc.* **1985**, *107*, 8103−8110.

10.1021/om000226a CCC: $20.00
Publication on Web 04/04/2001

Scheme 1

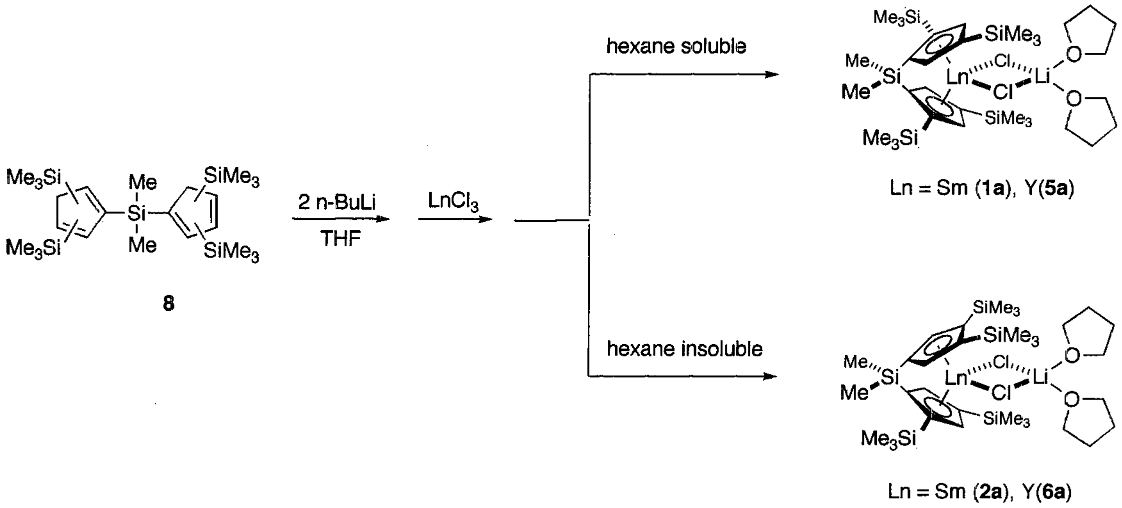

sitivity would be an obstacle for industrial use of the rare earth metal complexes, they are still promising olefin polymerization catalysts considering the advantage of being active without any aid of cocatalysts.

In addition to the fundamental investigations based on the use of bis-Cp* compounds mentioned above, modification of the cyclopentadienyl framework aiming for the improvement of the catalytic performance has also been carried out. Creating more open space around the metal center by connecting the two Cp* rings by a dimethylsilylene bridge has been shown to result in a higher ethylene polymerization activity.[2o] More importantly, iso-specific polymerization of 1-olefins was achieved by C_2 symmetric *ansa*-yttrocene [*rac*-$Me_2Si(2\text{-}Me_3Si\text{-}4\text{-}tBuC_5H_2)_2YH]_2$,[2j] which implies that the subtle steric factors imposed by substitution on the bridged Cp rings substantially influence the polymerization activity of this type of complex. Introduction of a chiral unit into the bridging group led to the isolation of a pure enantiomer of this type of complex,[2e] which was then used in an elegant study to establish the stereoselectivity of initial insertion steps in the iso-specific 1-olefin polymerization.[2d]

We have been interested in the relationship between the steric factors imposed by the substituents on the bridged Cp rings and the polymerization activity.[2a,b] Recently, we reported a detailed investigation on the relationship by using several divalent silylene-bridged samarium compounds.[2b] With the use of a variety of ligands with two connected Cp rings, we have succeeded in preparing four types of compounds: C_2 symmetric *rac*, $Me_2Si(2\text{-}Me_3Si\text{-}4\text{-}tBuC_5H_2)_2Sm(THF)_2$; C_1 symmetric, $Me_2Si[2,4\text{-}(Me_3Si)_2C_5H_2][3,4\text{-}(Me_3Si)_2C_5H_2]Sm(THF)_2$; *meso* with two bridging groups, $[1,2\text{-}(Me_2Si)(Me_2SiOSiMe_2)](4\text{-}Me_3CC_5H_2)_2Sm(THF)_2$; Ph_2Si-bridged C_{2v} symmetric, $Ph_2Si[2,4\text{-}(Me_3Si)_2C_5H_2][3,4\text{-}(Me_3Si)_2C_5H_2]Sm(THF)_2$. It was found in the study that in the series of divalent Sm complexes (i) the *meso* type exhibited the highest ethylene polymerization activity, (ii) the C_1 symmetric type gave the highest molecular weight polyethylene (M_n > 1 000 000), and (3) only the *rac* type was able to polymerize 1-olefins.

We have extended the investigation into trivalent rare earth metal complexes employing the same strategy used for the divalent Sm compounds. We report here the preparation of three types (*rac*, C_1, and *meso*) of trivalent Sm and Y complexes and the reactivity of the complexes bearing a $CH(SiMe_3)_2$ group toward olefin monomers.

Results and Discussion

Synthesis of *rac* and C_1 Type Rare Earth Halides [*rac*-Sm−Cl (1a), C_1-Sm−Cl (2a), $C_1(Ph_2Si)$−Sm−Cl (3), *rac*-Y−Cl (5a), and C_1-Y−Cl (6a)]. The ligand $Me_2Si[(Me_3Si)_2C_5H_3]$, **8**, consisting of Me_2Si-bridged Cp rings with two Me_3Si groups on each Cp ring, was used for the synthesis of both *rac* and C_1 type compounds. The reaction of $SmCl_3$ with a dilithium salt of **8** afforded a mixture of *rac*-Sm−Cl (**1a**) and C_1-Sm−Cl (**2a**). Although the structures of **1a** and **2a** differ only in the position of one of the Me_3Si groups in one Cp ring, the difference of their solubility is large enough for us to separate the two isomers. Hence, extraction with hexane led to the isolation of *rac* isomer **1a**, and extraction of the hexane-insoluble residue with ether gave C_1 symmetric isomer **2a**, as shown in Scheme 1.

The ^1H NMR spectrum of **1a** contains two Me_3Si resonances at 0.01 and −1.73 ppm, one Me_2Si resonance at 2.27 ppm, and two Cp-H resonances at 16.37 and 5.84 ppm, which clearly indicates C_2 symmetric character of **1a**. The same type of resonance pattern was observed for the divalent Sm compound *rac*-$Me_2Si(2\text{-}Me_3Si\text{-}4\text{-}tBuC_5H_2)_2Sm(THF)_2$.[2b] On the other hand, the ^1H NMR spectrum of **2a** contains four resonances (1.18, −0.54, −0.82, and −2.33 ppm) for Me_3Si groups, two resonances (2.97 and 1.14 ppm) for the bridging Me_2Si group, and four resonances (17.10, 10.35, 9.73, and 4.01 ppm) for Cp-Hs, which suggests that **2a** assumes a C_1 symmetric structure. This resonance pattern was observed for the C_1 symmetric divalent Sm complex $Me_2Si[2,4\text{-}(Me_3Si)_2C_5H_2][3,4\text{-}(Me_3Si)_2C_5H_2]Sm(THF)_2$, in which the two Me_3Si groups were located on the 2,4 positions in one Cp ring and the 3,4 positions in the other Cp ring.[2b]

The estimations from the ^1H NMR spectra were unambiguously verified by X-ray crystallographic analyses of **1a** and **2a** (Figures 1, 2, and Tables 1, 2), although only the connectivity of the atoms can be reliably

Table 1. Crystal Data for 1a, 2a, 2b, 3, and 7a

	1a	**2a**	**2b**	**3**	**7a**
formula	$C_{32}H_{62}Cl_2LiO_2Si_5Sm$	$C_{32}H_{62}Cl_2LiO_2Si_5Sm$	$C_{31}H_{65}Si_7Sm$	$C_{42}H_{66}Cl_2LiO_2Si_5Sm$	$C_{26}H_{48}ClO_2Si_5Y$
fw	847.52	847.52	784.85	971.66	657.45
cryst syst	triclinic	monoclinic	monoclinic	triclinic	orthorhombic
space group	*P*1	*P*2₁/*c*	*P*2₁/*c*	*P*1	*Pnma*
a/Å	12.611(4)	17.483(3)	17.385(4)	14.557(2)	15.950(5)
b/Å	17.109(3)	13.427(3)	10.03(1)	15.145(2)	17.862(5)
c/Å	12.134(4)	19.475(2)	24.744(4)	13.184(2)	12.495(5)
α/deg	99.74(3)	104.47(1)			
β/deg	115.16(2)	104.23(1)	91.94(2)	92.99(1)	
γ/deg	90.91(3)	83.17(1)			
V/Å^3	2324(1)	4431(1)	4311(3)	2793.8(7)	3559(1)
Z	2	4	4	2	4
D_{calcd}/(g cm^{-3})	1.211	1.270	1.209	1.155	1.227
F(000)	878	1756	1644	1006	1384
μ(Mo $K\alpha$)/cm^{-1}	15.33	16.08	15.77	12.83	19.03
no. of measd rflns	11 176	10 984	9278	13 333	4565
ratio of reflns/params	13.8	11.1	8.2	19.4	7.6
no. of obsd rflns ($I > 2.0\sigma(I)$)	4807	4320	2901	9252	1291
R^a (R_w)^b	0.123 (0.148)	0.075 (0.054)	0.097 (0.072)	0.058 (0.071)	0.096 (0.053)

^{a} $R = \sum||F_o| - |F_c||/\sum|F_o|$. ^{b} $R_w = (\sum w(|F_o| - |F_c|)^2/\sum w|F_o|^2)^{1/2}$; $w = 1/\sigma^2(F_o)$.

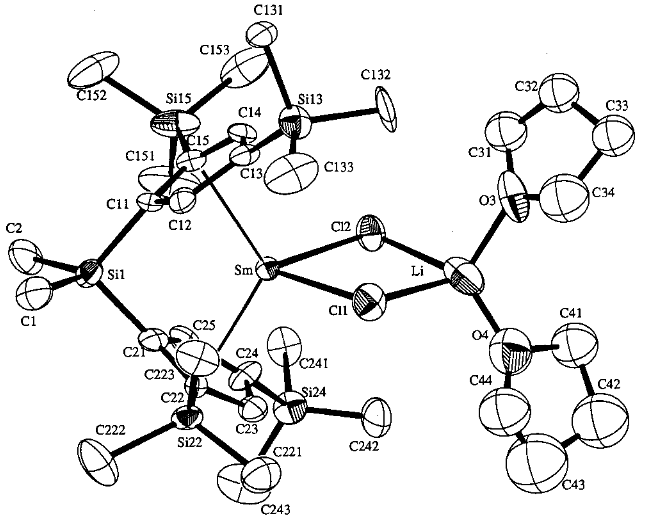

Figure 1. Structure of *rac*-Sm−Cl **1a**.

described for **1a** because of the poor quality of the data. The structure of **1a** is similar to that of the previously reported yttrium complex *rac*-$Me_2Si(2\text{-}Me_3Si\text{-}4\text{-}tBuC_5H_2)_2YCl_2Li(THF)_2$.[2j] Although it is not clear which factors determine the positions of Me_3Si groups on the two Cp rings, it is interesting to note that two bulky substitutents such as Me_3Si groups are located on adjoining carbons on the same Cp ring in **2a**, which seems to be highly sterically demanding. It is also noteworthy that the substantial difference of solubility between **1a** and **2a** arises from the difference of the position of just one Me_3Si group, as mentioned above. In **2a**, the (ring centroid)−metal−(ring centroid) angle is 116.3°, which is similar to the angles of Me_2Si-bridged divalent Sm complexes [*rac*-$Me_2Si(2\text{-}Me_3Si\text{-}4\text{-}tBuC_5H_2)_2Sm(THF)_2$, 115.8°; $(Me_2Si)(Me_2SiOSiMe_2)](4\text{-}Me_3CC_5H_2)_2Sm(THF)_2$, 116.5°][2b] and is about 20° smaller than that of the trivalent nonbridging Sm complex $(C_5Me_5)_2SmI(THF)$ (136(1)°, 137(1)°).[3]A Ph_2Si-bridged compound **9** was used for the complexation with $SmCl_3$. This ligand was designed in order to disfavor the location of bulky substituents on the 2,4 positions owing to steric repulsion with the Ph_2Si group. In the case of divalent Sm complexes, **9** afforded C_{2v} symmetric complex $Ph_2Si[3,4\text{-}(Me_3Si)_2C_5H_2]_2Sm(THF)_2$, which had all four Me_3Si groups on the 3 and 4 positions as expected.[2b,4] In contrast to the divalent Sm complex, the reaction of a dilithium salt of **9** with $SmCl_3$ led to the C_1 symmetric complex **3** according to Scheme 2. Because of the steric repulsion with the Ph_2Si group, the formation of the *rac*-type complex did not occur in this case. In addition, the formation of a C_{2v} type complex was also not observed. Thus, the use of the ligand **9** allows us to obtain the C_1 symmetric complex exclusively in this case. The ^1H NMR spectrum of **3** shows the typical resonance pattern of C_1 type complexes, and the precise structure was revealed by X-ray crystallography (Figure 3, Tables 1, 2). As summarized in Table 2, the important bond

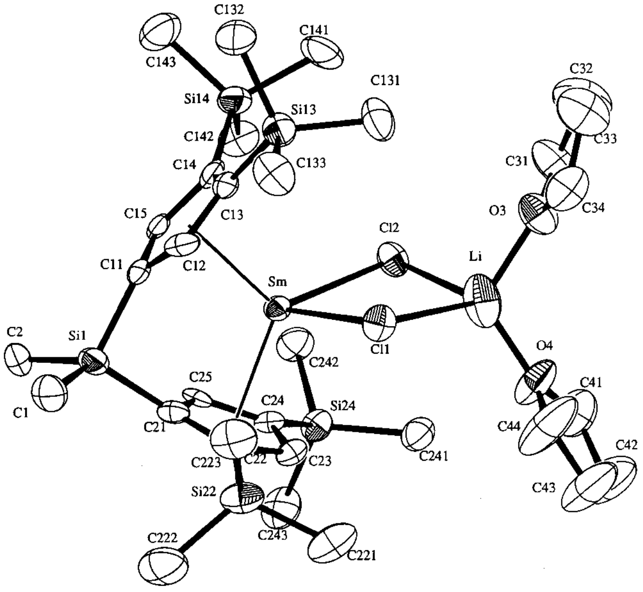

Figure 2. Structure of C_1-Sm−Cl **2a**.

---

(3) Evans, W. J.; Grate, J. W.; Levan, K. R.; Bloom, I.; Peterson, T. T.; Doedens, R. J.; Zhang, H.; Atwood, J. L. *Inorg. Chem.* **1986**, *25*, 3614−3619.

(4) Because of the highly fluxional character of the Si−C(Cp) bonds, movement of Me_3Si groups on Cp rings occurred during the transformation from **9** to **3** so as to form the thermodynamically stable complex. For the fluxionality of silyl groups on the Cp ring, see: Jutzi, P. *Chem. Rev.* **1986**, *86*, 983−996.

Scheme 2

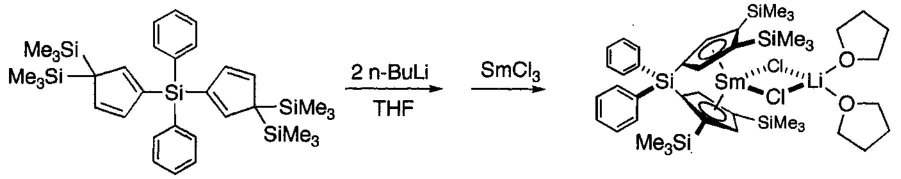

9 **3**

Table 2. Selected Bond Lengths (Å) and Angles (deg) for 1a, 2a, 2b, and 3[a]

	1a	**2a**	**2b**	**3**
	Bond Lengths[b]			
C(11)−C(12)	1.40(4)	1.43(2)	1.46(4)	1.416(9)
C(12)−C(13)	1.48(4)	1.42(2)	1.45(4)	1.41(1)
C(13)−C(14)	1.44(4)	1.41(2)	1.50(4)	1.428(9)
C(14)−C(15)	1.39(4)	1.43(2)	1.42(4)	1.404(10)
C(15)−C(11)	1.52(4)	1.41(2)	1.42(4)	1.413(9)
C(21)−C(22)	1.46(4)	1.43(2)	1.47(4)	1.46(1)
C(22)−C(23)	1.47(4)	1.42(2)	1.48(3)	1.41(1)
C(23)−C(24)	1.48(4)	1.41(2)	1.36(3)	1.416(10)
C(24)−C(25)	1.38(4)	1.41(2)	1.39(3)	1.41(1)
C(25)−C(21)	1.42(3)	1.42(2)	1.49(4)	1.421(9)
C(13)−Si(13)	1.83(3)	1.89(1)	1.88(3)	1.882(7)
C(14)−Si(14)	1.88(1)	1.88(3)	1.889(8)	
C(15)−Si(15)	1.81(3)			
C(22)−Si(22)	1.88(3)	1.88(1)	1.87(3)	1.877(7)
C(24)−Si(24)	1.85(2)	1.86(1)	1.93(2)	1.858(7)
Si(1)−C(11)	1.87(3)	1.85(2)	1.83(3)	1.872(7)
Si(1)−C(21)	1.86(3)	1.84(1)	1.80(3)	1.869(8)
Si(1)−C(1)	1.92(3)	1.86(2)	1.84(2)	1.872(8)
Si(1)−C(2)	1.92(4)	1.84(1)	1.83(3)	1.877(7)
Sm−Cl(1)	2.708(8)	2.698(4)		2.678(2)
Sm−Cl(2)	2.705(7)	2.694(4)		2.668(2)
Sm−Cp(1)	2.45	2.44	2.57	2.445
Sm−Cp(2)	2.45	2.44	2.42	2.447
C[Cp(1)]−Sm(av)	2.74	2.72	2.81	2.724
C[Cp(2)]−Sm(av)	2.74	2.73	2.71	2.729
Sm−C(3)			2.47(2)	
Sm−C(7)[b]			2.84(3)[b]	
C(3)−Si(2)			1.85(3)	
C(3)−Si(3)			1.83(2)	
	Bond Angles			
[Cp(1) centroid]−Sm−[Cp(2) centroid]	119.7	116.3	117.1	118.9
C(11)−Si(1)−C(21)	99(1)	98.1(7)		101.0(3)
C(1)−Si(1)−C(2)	108(1)	106.1(7)	107(1)	106.6(3)
Cl(1)−Sm−Cl(2)	84.8(2)	83.4(1)		83.88(6)
Sm−C(3)−Si(2)			137(1)	
Sm−C(3)−Si(3)			98(1)	
Si(2)−C(3)−Si(3)			115(1)	
C(3)−Si(3)−C(7)			106(1)	
C(3)−Si(3)−C(8)			115(1)	
C(3)−Si(3)−C(9)			114(1)	

[a] Cp(1) and Cp(2) are the Cp rings consisting of C(11), C(12), C(13), C(14), C(15) and C(21), C(22), C(23), C(24), C(25), respectively. [b] Sm−C(7) an intramolecular interaction.

lengths and angles in **3** are similar to those in C_1-Sm−Cl (**2a**), which means that the change of the bridging group from Me_2Si to Ph_2Si does not affect the structure of the complexes, at least in the solid state.

The same synthetic procedure can be applied for the synthesis of *rac* and C_1 type yttrium halides (**5a** and **6a**) as shown in Scheme 1. The yttrium compounds show the similar difference of solubility, which enables us to separate them into pure isomers. The structures of **5a** and **6a** were confirmed from their ^{1}H NMR spectra, whose resonance patterns were analogous to those of **1a** and **2a**, respectively, although the chemical shift of the resonances were in a reasonable range shifted, reflecting the diamagnetic character of the yttrium element.

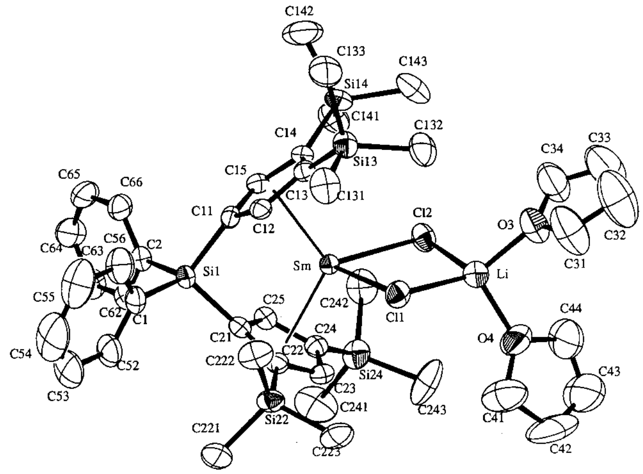

Figure 3. Structure of C_1(Ph$_2$Si)−Sm−Cl **3**.

Synthesis of *meso* Type Rare Earth Halides [*meso*-Sm−Cl (4a) and *meso*-Y−Cl (7a)]. We have already found that the C_s symmetric *meso* type divalent Sm complex, in which two Cp rings are connected by two different bridging groups, Me_2Si and $Me_2SiOSiMe_2$, can be obtained from the ligand **10**.[2b] The syntheses of trivalent *meso* type Sm and Y complexes were attempted by using this type of ligand. The reaction of $SmCl_3$ with the dilithium salt of **10** afforded *meso* type Sm halide **4a** according to Scheme 3. In the ^{1}H NMR spectrum of **4a**, the presence of three resonances for the bridging MeSi groups in 2:2:1 integral ratio, together with one and two resonances for t-Bu and Cp-H respectively, indicated the C_s symmetric structure of the complex. The same resonance pattern was observed in the ^{1}H NMR spectrum of *meso* type divalent Sm complex [1,2-(Me$_2$Si)(Me$_2$SiOSiMe$_2$)](4-Me$_3$CC$_5$H$_2$)$_2$Sm(THF)$_2$, which was further characterized by X-ray diffraction.[2b]

In a similar manner, *meso* type yttrium halide **7a** was obtained from YCl_3 and a dilithium salt of Me$_3$Si-substituted doubly bridged compound **11**, as shown in Scheme 4. The ^{1}H NMR spectrum of **7a** contains two sets of resonances characteristic of *meso* type structure in an almost 1:1 ratio, although the structural difference of the two species in solution is not clear. Compared to Sm analogue **4a**, the integral ratio of coordinated THF molecules indicated that the molar ratio of THF to the ligand moiety was 1:1 in the spectrum. The structure of **7a** in the solid state was revealed by a single-crystal X-ray diffraction study, and the ORTEP drawing is shown in Figure 4 and selected bond lengths and angles are listed in Table 3. As expected from the ^{1}H NMR spectrum, only one THF molecule is coordinated to the Y center along with the coordination of a Cl anion. It is clearly shown that **7a** has a C_s symmetric *meso* type structure in which a mirror plane including Y, Cl, O(3), Si(1), O(1), C(1), and C(2) bisects the whole molecule.

Scheme 3

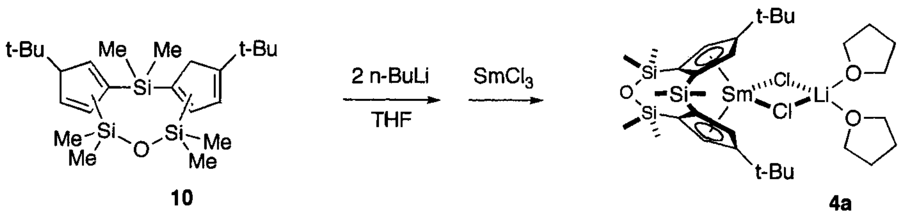

Scheme 4

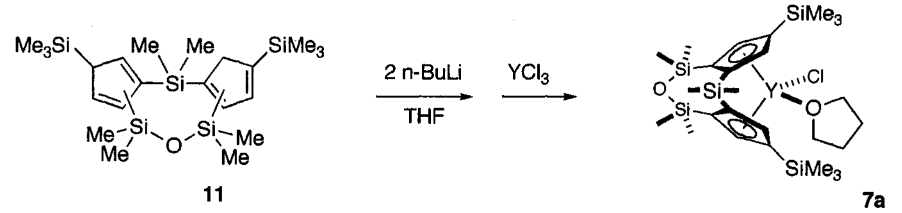

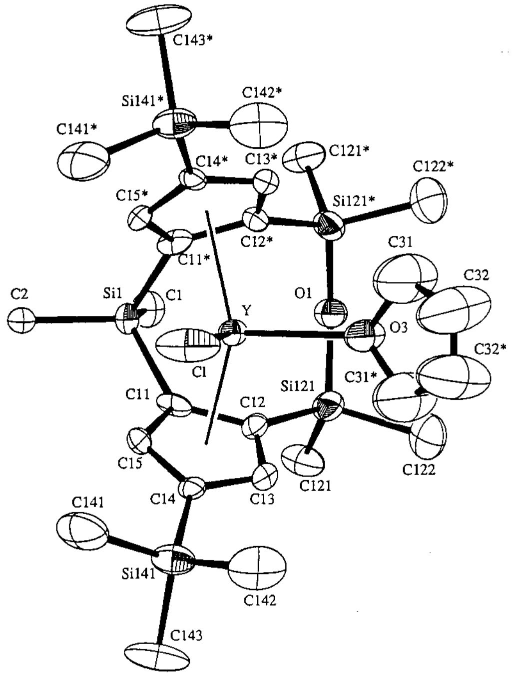

Figure 4. Structure of *meso*-Y−Cl **7a**.

Table 3. Selected Bond Lengths (Å) and Angles (deg) for 7a[a]

Bond Lengths	
C(11)−C(12)	1.43(2)
C(12)−C(13)	1.42(2)
C(13)−C(14)	1.44(2)
C(14)−C(15)	1.41(2)
C(15)−C(11)	1.39(2)
C(14)−Si(141)	1.87(1)
C(11)−Si(1)	1.89(1)
C(12)−Si(121)	1.83(1)
Si(121)−O(1)	1.634(5)
Si(1)−C(1)	1.86(2)
Si(1)−C(2)	1.80(2)
Y−Cl	2.541(8)
Y−O(3)	2.35(2)
Y−Cp(1)	2.38
Bond Angles	
[Cp(1) centroid]−Y−[Cp(1*) centroid]	120.8
C(11)−Si(1)−C(11*)	96.1(6)
C(1)−Si(1)−C(2)	107.2(10)
Cl−Y−O(3)	89.7(5)
C(12)−Si(121)−O(1)	110.4(6)
Si(121)−O(1)−Si(121*)	145.3(8)

[a] Cp(1) and Cp(1*) are the Cp rings consisting of C(11), C(12), C(13), C(14), C(15) and C(11*), C(12*), C(13*), C(14*), C(15*), respectively.

The (ring centroid)−Y−(ring centroid) angle in **7a** is 120.8°, which is ca. 11−14° smaller than those of nonbridging bis-Cp Y complexes, $Cp^*_2YCH(SiMe_3)_2$ (134.4(4)°) and $Cp^*_2YN(SiMe_3)_2$ (132.2(2)°, 132.4(2)°).[5]

Synthesis of Rare Earth Metal Alkyl Complexes with Bridging Bis-Cp Ligands. It has been reported that bis-Cp type rare earth halides can be effectively converted to the neutral alkyl derivatives by the reaction with $MCH(SiMe_3)_2$ (M = Li, K).[2n,o,5,6] The steric bulkiness of the $CH(SiMe_3)_2$ moiety prevents the coordination of Lewis basic compounds such as THF or ether and the formation of ate compounds by the attack of the anionic group to the highly electrophilic metal center. In addition, β-alkyl elimination, which has been frequently observed as a decomposition pathway of electrophilic early transition metal complexes, can be hampered because the high-energy Si=C bond should be formed by the elimination.[2n] Hence, we conducted transformation of the rare earth halides prepared above (**1a**, **2a**, **3**, **4a**, **5a**, **6a**, **7a**) to the alkyl complexes by the reaction with $LiCH(SiMe_3)_2$.

In the similar manner reported for bis-Cp type complexes,[2n,4,5] the reaction of the halides (**1a**, **2a**, **4a**, **5a**, **6a**, **7a**) with an ether solution of $LiCH(SiMe_3)_2$ in toluene at 23 °C proceeded smoothly to give alkyl complexes (**1b**, **2b**, **4b**, **5b**, **6b**, **7b**) after recrystallization from hexane according to Scheme 5. However, for the Ph_2Si-bridged halide **3**, the alkyl complex was obtained only as a crude powder, and we have not succeeded in isolating the complex in a pure form. In the NMR spectra of the *rac* and *meso* type complexes, two Cp rings became nonequivalent by the introduction of the alkyl group, which was the reported phenomenon for other symmetric bis-Cp type rare earth complexes.[2n,4,5] In the

---

(5) Haan, K. H.; Boer, J. L.; Teuben, J. H.; Spek, A. L.; Kojic-Prodic, B.; Hays, G. R.; Huis, R. *Organometallics* **1986**, *5*, 1726−1733.

(6) (a) Schumann, H.; Rosenthal, E. C. E.; Kocio-Köhn, Molander, G. A.; Winterfeld, J. *J. Organomet. Chem.* **1995**, *496*, 233−240. (b) Giardello, M. A.; Conticello, V. P.; Brard, L.; Sabat, M.; Rheingold, A. L.; Stern, C. L.; Marks, T. J. *J. Am. Chem. Soc.* **1994**, *116*, 10212−10240. (c) Schumann, H.; Esser, L.; Loebel, J.; Dietrich, A.; Helm, D.; Ji, X. *Organometallics* **1991**, *10*, 2585−2592. (d) Heeres, H. J.; Renkema, J.; Booij, M.; Meetsma, A.; Teuben, J. H. *Organometallics* **1988**, *7*, 2495−2502.

Scheme 5

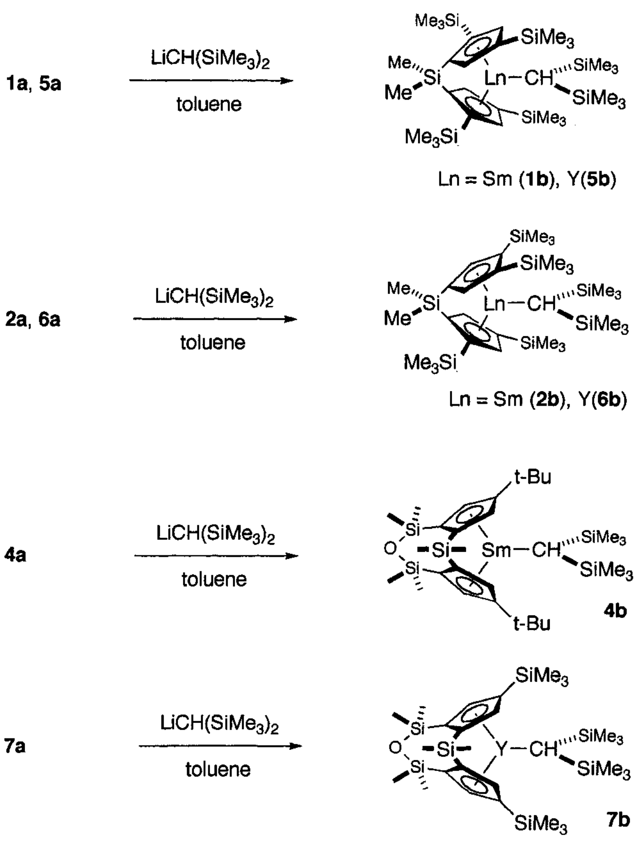

^{13}C NMR spectra of yttrium alkyl complexes **5b** and **7b**, a clear ^{1}J coupling was observed between ^{89}Y and the α-carbon of the alkyl group. The coupling constants for **5b** (31.9 Hz) and **7b** (32.8 Hz) are similar to the reported values for Cp*$_2$YCH(SiMe$_3$)$_2$ (36.6 Hz)[4] and (C$_5$Me$_4$-Et)$_2$YCH(SiMe$_3$)$_2$ (35 Hz).[5a]

Structure of Me$_2$Si[2,4-(Me$_3$Si)$_2$C$_5$H$_2$][3,4-(Me$_3$Si)$_2$-C$_5$H$_2$]SmCH(SiMe$_3$)$_2$ (2b). The structure of *rac*-Sm–R (**2b**) was precisely determined by a single-crystal X-ray diffraction study (Figure 5 and Tables 1, 2). The four Me$_3$Si groups on the ligand are located at the 3,4 and 2,4 positions on the Cp rings in the same manner as the starting halide **2a**, which indicates that the transformation with LiCH(SiMe$_3$)$_2$ did not affect the ligand framework with respect to the positions of the substituents on the Cp rings. The Sm–C(3) bond distance, 2.47(2) Å, is unexceptional compared to the distances of analogous complexes (*R*)-Me$_2$Si(C$_5$Me$_4$)[(−)-menthyl-Cp]SmCH(SiMe$_3$)$_2$] (**12**) (2.504(7), 2.487(7) Å)[5b] and (C$_5$Me$_4$Et)$_2$SmCH(SiMe$_3$)$_2$ (**13**) (2.502(3) Å).[5a]

As has always been observed in other rare earth alkyl complexes with the CH(SiMe$_3$)$_2$ group, one of the two Me$_3$Si groups approaches the Sm center at an acute Ln–Cα–Siβ angle in the solid state.[4,5] The Sm–C(3)–Si(3) angle is 98(1)°, which is 39° smaller than the other angle, Sm–C(3)–Si(2) 137(1)°. This phenomenon has been ascribed to the interaction between the metal center and the electron density of the Siβ–Cγ bond in order to compensate the high electron deficiency of the metal center.[5b] In accord with the presence of the interaction, the location of one of the Me groups on Si(3) is close to the Sm center [Sm–C(7), 2.84(3) Å], forming a pseudo-metalacyclobutane conformation [cf. Sm–C(6), 4.62(3) Å]. The distance is also comparable to the corresponding bond lengths in **12** (2.865(7), 2.998(6) Å)[5b] and **13** (2.953 Å).[5a] In addition, the Cα–Siβ–Cγ angle with the γ-carbon interacting with Sm [C(3)–Si(3)–C(7), 106(1)°] is significantly smaller than the other two angles [C(3)–Si(3)–C(8), 115(1)°; C(3)–Si(3)–C(9), 114(1)°]. It is also interesting to note that the Sm–Cγ interaction exists in the more sterically crowded side on the equatorial girdle with two Me$_3$Si groups on the 4 position on both Cp rings. As a result, the more sterically demanding side of the CH(SiMe$_3$)$_2$ group is oriented toward the less sterically crowded side in the equatorial girdle, as is clearly seen from the top view of **2b** (Figure 5, bottom). The same kind of orientation of the CH(SiMe$_3$)$_2$ group has been observed in **12** and related complexes.[5b]

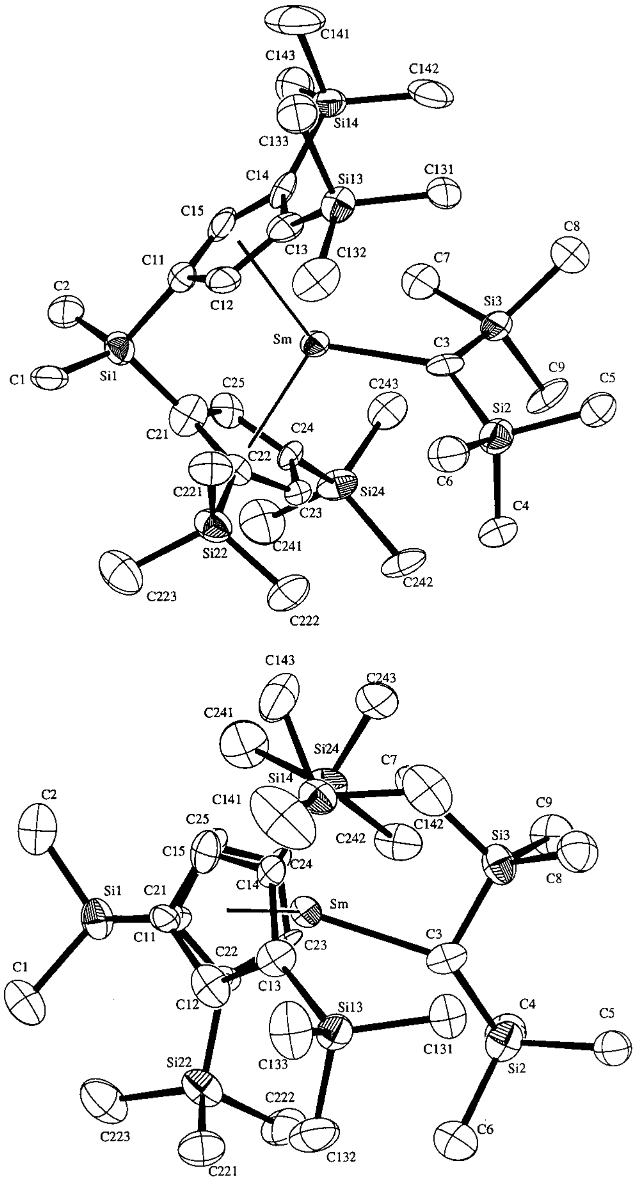

Figure 5. Structure of C_1-Sm–R **2b**.

Another structural point of interest in **2b** is the difference of the average C(Cp)–Sm distances for the two Cp rings. There is a significant difference between the distance on Cp with Me$_3$Si on the 3,4 positions (2.81 Å) and that with Me$_3$Si on the 2,4 positions (2.71 Å). The longer C(Cp)–Sm distance on the former Cp ring suggests that high steric crowding exists around the Cp

Scheme 6

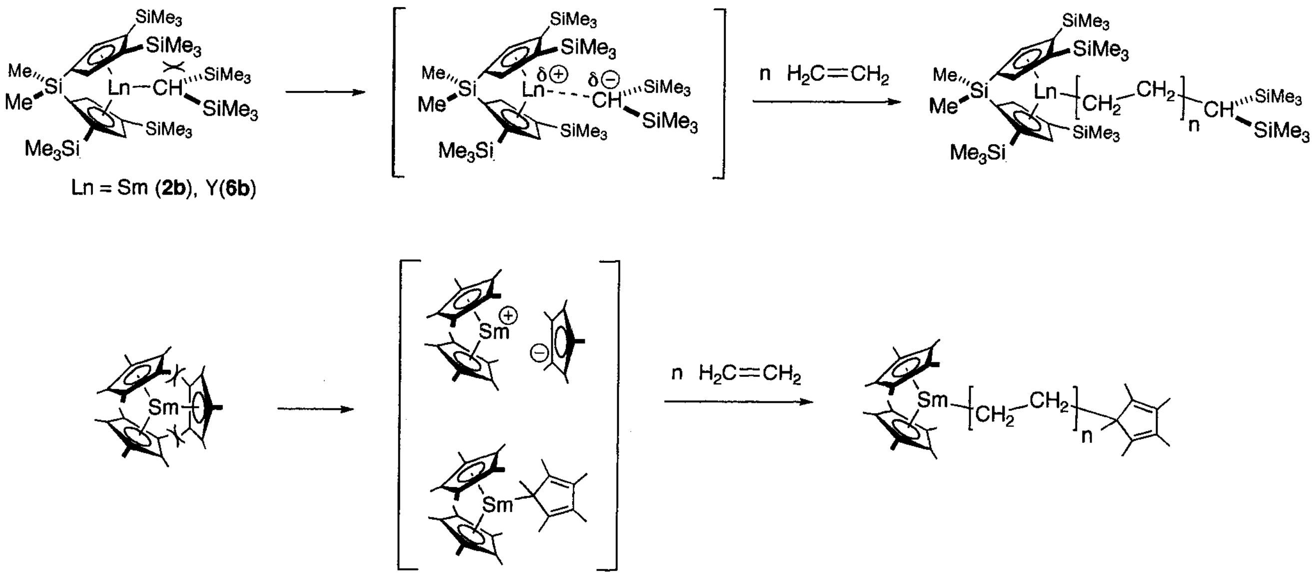

ring owing to the presence of the two adjoining Me_3Si groups on the Cp ring. Because of the steric crowding, two of the Sm–C(Cp) distances [Sm–C(13), 2.88(3) Å, Sm–C(14), 2.92(3) Å] are even longer than the Sm–C(7) distance of the agostic interaction (2.84(3) Å). The steric effect will be related with the reactivity of the complexes with olefins in the next section.

Olefin Polymerization by Rare Earth Alkyl Complexes. It is generally considered that the $CH(SiMe_3)_2$ group on rare earth metal complexes is more useful as a precursor to generate hydride derivatives than as an initiating group for olefin polymerization.[2n,o] Although the steric bulkiness is essential to prevent the undesirable coordination of Lewis basic compounds, it may also prevent the approach and coordination of olefin molecules to the metal center, which should precede the initiation and propagation of the polymerization. Accordingly, in contrast to the very high ethylene polymerization activity of $(Cp^*_2LnH)_2$ (Ln = La, Nd), $Cp^*_2LnCH(SiMe_3)_2$ was reported to be completely inactive for the polymerization.[2n] However, owing to the intrinsic high reactivity, rare earth hydride derivatives are more difficult to handle than alkyl derivatives. For example, we have observed that $(Cp^*_2SmH)_2$ decomposes slowly at 23 °C in toluene under a complete argon atmosphere. On the other hand, stabilized by the Ln–Cγ interaction, rare earth alkyl compounds bearing $CH(SiMe_3)_2$ groups in this study did not show any decomposition for several months in benzene-d_6 solution at 23 °C. Thus, to explore the possibility of using the stable alkyl complexes as initiators for olefin polymerization, we examined the reactivity of alkyl derivatives **1b**, **2b**, **4b**, **5b**, **6b**, and **7b** toward olefin monomers.

As summarized in Table 4, it was found that C_1 symmetric alkyl derivatives **2b** and **6b** polymerized ethylene at 23 °C in toluene with ethylene pressure of 1 atm. In contrast, no evidence of ethylene polymerization was observed for C_2 and C_s symmetric complexes (**1b**, **4b**, **5b**, and **7b**) in the same condition. The activity for yttrium complex **6b** is higher than samarium complex **2b**, reaching 186 000 gPE/mol·h·atm. The molecular weight of the polyethylene obtained by **6b**, which is more than 300 000, is also higher than that obtained by **2b**. The molecular weight distributions of the polyethylenes are relatively narrow (M_w/M_n = 1.6–2.3).

Table 4. Ethylene Polymerization by Trivalent Rare Earth Alkyl Complexes[a]

initiator	react period, min	activity, 10^{-4} g of PE/(mol h)	$10^{-4}M_n$	M_w/M_n
rac-Sm–R **1b**		no polymerization		
C_1-Sm–R **2b**	3	2.92	7.46	2.07
	5	3.08	9.96	1.84
	10	2.43	15.2	2.01
meso-Sm–R **4b**		no polymerization		
rac-Y–R **5b**		no polymerization		
C_1-Y–R **6b**	1	18.6	33.1	1.65
	3	7.4	31.9	2.31
meso-Y–R **7b**		no polymerization		

[a] Reaction conditions: temperature, 23 °C; initiator concentration, 1.0 mM; solvent, toluene; ethylene pressure, 1 atm.

It is interesting to note that the ethylene polymerization activity was observed only on C_1 symmetric complexes (**2b**, **6b**), which had the most sterically crowded environment around the metal center because of the presence of three Me_3Si groups on the 3,4 positions on the Cp rings. Recently, it was reported that the unusually high reactivity of Cp^*_3Sm can be ascribed to the high steric crowding around the metal center by comparison of the reactivities and crystal structures of Cp^*_3Sm and $Me_2Si(C_5Me_4)_2SmCp^*$.[6] The less crowded nature of the latter complex was confirmed by the normal Sm–C(Cp*) bond distances, whereas the bond distances on Cp^*_3Sm have been found to be extremely long.[7] It was concluded that because of the steric crowding, one of the Cp* could not form a stable bond with the metal center and ethylene could insert into the unstable Sm–C(Cp*) bond. We believe that the same theory can be applied in the case of our C_1 type rare earth alkyl complexes **2b** and **6b**. The aforementioned difference of Sm–C(Cp) distances in **2b** indicates that high steric crowding exists around the metal center in these C_1 symmetric complexes. Although the Sm–

---

[7] Evans, W. J.; Cano, D. A.; Greci, M. A.; Ziller, J. W. *Organometallics* **1999**, *18*, 1381–1388.

Table 5. 1-Olefin Polymerization by C_1-Y−R (6b)[a]

monomer	react temp, °C	react period, h	$10^{-4}M_n$	M_w/M_n
1-pentene	23	3	1.60	1.42
1-hexane	23	3	2.54	1.63
	23	6	3.11	1.82
	0	3	6.45	1.20

[a] Reaction conditions: neat; initiator concentration, 0.2 mol %.

$C[CH(SiMe_3)]_2$ distance is normal, the Sm−C bond should be perturbed in solution by free rotations of C(Cp)−Si bonds on the 3,4 positions on the Cp rings. The free rotation in solution is confirmed by the sharp singlet resonances for the Me_3Si groups in the ^1H NMR of **2b** and **6b**. In such a manner, the $Sm-C[CH(SiMe_3)]_2$ bond could be lengthened or possesses ionic character, which would result in a high activity for ethylene insertion.In addition to ethylene, 1-olefins such as 1-pentene and 1-hexane were polymerized by a C_1 symmetric alkyl complex of yttrium, **6b** (Table 5). Although the reactivity was very low and polymers were obtained in a trace yield, GPC analysis indicated the poly(1-hexane) obtained by the reaction at 0 °C had a high molecular weight ($M_n = 64\,500$) and a narrow molecular weight distribution ($M_w/M_n = 1.20$).

In conclusion, we have demonstrated that a series of bridging bis(cyclopentadienyl) ligands employed in this study are very useful to prepare a variety of rare earth metal metallocene complexes with different steric environments around the metal center. The steric factors strongly influence the reactivity of the Ln−C bond of the alkyl derivatives, resulting in the high ethylene insertion activity in the C_1 type complex.

Experimental Section

General Considerations. All operations were performed under argon by using standard Schlenk techniques. Tetrahydrofuran (THF), hexane, and diethyl ether (ether) were dried over Na/K alloy and distilled before use. Toluene was dried over Na and distilled before use. Toluene used for polymerization was dried over Na/K alloy and thoroughly degassed by trap-to-trap distillation. Ethylene (Nakamura Oxygen Co.) was used without further purification. 1-Pentene and 1-hexene were dried over Na/K alloy and distilled before use. $ClMe_2OSiOMe_2Cl$ (ShinEtsu Silicon Chemicals) was dried over NaH and used without further purification. The preparation of all the ligands used in this study except for **10** was already reported.[2b] $SmCl_3$ and YCl_3 were prepared by the reactions of Ln_2O_3 (Shiga Rare Metals & Chemicals Co.) and excess NH_4Cl in concentrated HCl at 100 °C followed by removal of excess NH_4Cl by sublimation at 360 °C/0.1 mmHg. ^1H NMR spectra were recorded on a Bruker AMX 400wb spectrometer (400.14 MHz) or JEOL JNM-LA 400 (395.75 MHz) spectrometer in sealed tubes at ambient probe temperature. ^{13}C NMR spectra were recorded on a JEOL JNM-LA 400 (99.45 MHz) spectrometer in sealed tubes at ambient probe temperature. ^1H and ^{13}C chemical shifts are reported versus $SiMe_4$ and were determined by reference to the residual ^1H and ^{13}C solvent peaks. Complexometric metal analyses were conducted by the method reported by Atwood and Evans.[8] (The analyses did not give satisfactory results in two cases, probably because of the high air sensitivity of the complexes.) M_w and M_w/M_n values of poly(1-pentene) and poly(1-hexene) were determined by gel permeation chromatography (GPC) on a Tosoh SC-8010 using TSKgel G2000, G3000, G4000, and G5000 columns in chloroform at 40 °C. M_w and M_w/M_n values of polyethylene were determined by GPC on a Waters 150C using a Shodex AT806MS column in 1,2,4-trichlorobenzene at 140 °C. M_w and M_w/M_n were calibrated from standard polystyrene.

Structure Solution and Refinement for Complexes 1a, 2a, 2b, 3, and 7a. All diffraction measurements was performed on a Rigaku AFC-5R diffractometer with graphite-monochromated Mo Kα radiation. Since the complexes were highly air-sensitive, crystals were sealed in a thin-walled glass capillary tube under an argon atmosphere. The X-ray data were collected at room temperature using the $\omega-2\theta$ scan technique to a maximum 2θ value of 55.0° for **1a**, **2a**, **3**, and **7a**, and 52.0° for **2b**. The intensity data were corrected for conventional Lorentz and polarization effects and absorption based on a series of azimuthal scans.

The non-hydrogen atoms were refined anisotropically by full-matrix least-squares methods except for the carbon atoms of THF ligands in **1a**, which were refined isotropically. The hydrogen atoms were fixed at their standard geometries and were not refined. The carbon atoms of THF ligands in all the complexes seem to be disordered. However, since the attempts to locate these carbon atoms into two separate positions were unsuccessful, the THF ligands are described as having planar conformation consisting of the carbon atoms with large thermal vibrational parameters. All calculations were performed by the use of the teXsan crystallographic software package (teXsan: Crystal Structure Analysis Package, Molecular Structure Corp. [1985 and 1999]).

Preparation of *rac*-$Me_2Si[2,4\text{-}(Me_3Si)_2C_5H_2]_2SmCl_2Li(THF)_2$ (1a) and $Me_2Si[2,4\text{-}(Me_3Si)_2C_5H_2][3,4\text{-}(Me_3Si)_2C_5H_2]SmCl_2Li(THF)_2$ (2a). A solution of the ligand **8** (2.00 g, 4.19 mmol) in THF (25 mL) was cooled to 0 °C. nBuLi (1.60 M solution in hexane, 5.3 mL, 8.5 mmol) was added to the solution dropwise, and the mixture was stirred and warmed to 23 °C gradually over 6 h. The resulting solution of the lithium dianion of **8** was added to a suspension of $SmCl_3$ (1.15 g, 4.48 mmol) in THF (20 mL), and the mixture was refluxed for 11 h. After the solvent was removed by evaporation, the residual solid was dried under vacuum. Hexane (80 mL) was added to the solid, and the resulting suspension was stirred for 15 h at 23 °C. The suspension was separated into a yellow supernatant and a hexane-insoluble solid by centrifugation. After a part of the hexane was removed from the supernatant under reduced pressure, by cooling the resulting concentrated solution at −20 °C, **1a** was obtained as yellow crystals (0.88 g, 1.0 mmol, 25%). Ether (20 mL) was added to the hexane-insoluble solid mentioned above, and the suspension was stirred at 23 °C for 2 days. A yellow ether solution was obtained by centrifugation, and recrystallization of the solution at −20 °C afforded **2a** as yellow crystals (0.78 g, 0.92 mmol, 22%).

***rac*-$Me_2Si[2,4\text{-}(Me_3Si)_2C_5H_2]_2SmCl_2Li(THF)_2$ (1a).** ^1H NMR (400.14 MHz, C_6D_6): δ 16.37 (s, 2H, Cp-H), 5.84 (s, 2H, Cp-H), 4.76 (s, 8H, THF-α), 2.27 (s, 6H, Me_2Si), 2.01 (s, 8H, THF-β), 0.01 (s, 18H, Me_3Si), −1.73 (s, 18H, Me_3Si). Anal. Calcd for $C_{32}H_{62}Cl_2LiO_2Si_5Sm$: Sm, 17.74. Found: Sm, 17.94.

$Me_2Si[2,4\text{-}(Me_3Si)_2C_5H_2][3,4\text{-}(Me_3Si)_2C_5H_2]SmCl_2Li(THF)_2$ (2a). ^1H NMR (400.14 MHz, C_6D_6): δ 17.10 (s, 1H, Cp-H), 10.35 (s, 1H, Cp-H), 9.73 (s, 1H, Cp-H), 4.43 (s, 8H, THF-α), 4.01 (s, 1H, Cp-H), 2.97 (s, 3H, Me_2Si), 1.85 (s, 8H, THF-β), 1.18 (s, 9H, Me_3Si), 1.14 (s, 3H, Me_2Si), −0.54 (s, 9H, Me_3Si), −0.82 (s, 9H, Me_3Si), −2.33 (s, 9H, Me_3Si). Anal. Calcd for $C_{32}H_{62}Cl_2LiO_2Si_5Sm$: Sm, 17.74. Found: Sm, 17.90.

***rac*-$Me_2Si[2,4\text{-}(Me_3Si)_2C_5H_2]_2SmCH(SiMe_3)_2$ (1b).** A solution of **1a** (0.80 g, 0.94 mmol) in toluene (50 mL) was placed in a Schlenk tube and cooled to 0 °C. $(Me_3Si)_2CHLi$ (0.54 M solution in ether, 2.6 mL, 1.4 mmol) was added to the solution dropwise, and the mixture was stirred and warmed to 23 °C

---

(8) Evans, W. J.; Gonzales, S. L.; Ziller, J. W. *J. Am. Chem. Soc.* **1991**, *113*, 7423.

(9) Atwood, J. L.; Hunter, W. E.; Wayda, A. L.; Evans, W. J. *Inorg. Chem.* **1981**, *20*, 4115−4119.

gradually over 12 h. After the solvent was removed by evaporation, the residual solid was dried under vacuum. Hexane (40 mL) was added to the solid, and the resulting suspension was stirred at 23 °C for 12 h. The hexane-insoluble solid was removed by centrifugation. After a part of the hexane was removed from the supernatant under reduced pressure, by cooling the resulting concentrated solution at −20 °C, **1b** was obtained as red crystals (0.20 g, 0.25 mmol, 27%). ^{1}H NMR (400.14 MHz, C_6D_6): δ 17.65 (s, 1H, Cp-H or SmC*H*($SiMe_3$)$_2$), 16.66 (s, 1H, Cp-H or SmC*H*($SiMe_3$)$_2$), 16.49 (s, 1H, Cp-H or SmC*H*($SiMe_3$)$_2$), 10.34 (s, 1H, Cp-H or SmC*H*($SiMe_3$)$_2$), 3.76 (s, 3H, Me_2Si), 1.74 (s, 3H, Me_2Si), 0.25 (s, 9H × 2, Me_3Si), 0.10 (s, 9H, Me_3Si), −0.29 (s, 9H, Me_3Si), −1.77 (s, 9H, Me_3Si), −3.10 (s, 9H, Me_3Si). One of the Cp-H or SmC*H*($SiMe_3$)$_2$ signals was obscured by the other resonances. Anal. Calcd for $C_{31}H_{65}Si_7Sm$: Sm, 19.16. Found: Sm, 18.90.

$Me_2Si[2,4\text{-}(Me_3Si)_2C_5H_2][3,4\text{-}(Me_3Si)_2C_5H_2]SmCH(SiMe_3)_2$ (2b). **2a** was prepared by using the procedure reported above for **1b** with **2a** (1.44 g, 1.70 mmol), $(Me_3Si)_2CHLi$ (0.83 M solution in ether, 2.5 mL, 2.1 mmol), and toluene (50 mL). **2a** was obtained as red crystals (0.926 g, 1.18 mmol, 69.4%). ^{1}H NMR (400.14 MHz, C_6D_6): δ 17.83 (s, 1H, Cp-H or SmC*H*($SiMe_3$)$_2$), 17.35 (s, 1H, Cp-H or SmC*H*($SiMe_3$)$_2$), 13.15 (s, 1H, Cp-H or SmC*H*($SiMe_3$)$_2$), 12.27 (s, 1H, Cp-H or SmC*H*($SiMe_3$)$_2$), 3.80 (s, 3H, Me_2Si), 0.83 (s, 3H, Me_2Si), 0.75 (s, 9H, Me_3Si), −0.22 (s, 9H, Me_3Si), −0.53 (s, 9H, Me_3Si), −0.55 (s, 9H, Me_3Si), −3.05 (s, 9H, Me_3Si), −7.29 (s, 9H, Me_3Si). One of the Cp-H or SmC*H*($SiMe_3$)$_2$ signals was obscured by the other resonances. Anal. Calcd for $C_{31}H_{65}Si_7Sm$: Sm, 19.16. Found: Sm, 18.95.

$Ph_2Si[2,4\text{-}(Me_3Si)_2C_5H_2][3,4\text{-}(Me_3Si)_2C_5H_2]SmCl_2Li(THF)_2$ (3). A solution of the ligand **9** (12.10 g, 20.13 mmol) in THF (60 mL) was cooled to 0 °C. nBuLi (1.63 M solution in hexane, 24.6 mL, 40.1 mmol) was added to the solution dropwise, and the mixture was stirred and warmed to 23 °C gradually over 6 h. The resulting solution of the lithium dianion of **9** was added to a suspension of $SmCl_3$ (5.15 g, 20.1 mmol) in THF (60 mL), and the mixture was refluxed for 12 h. After the solvent was removed by evaporation, the residual solid was dried under vacuum. Hexane (80 mL) was added to the solid, and the resulting suspension was stirred for 15 h at 23 °C. A hexane-insoluble solid was removed by centrifugation. After a part of the hexane was removed from the supernatant under reduced pressure, and cooling the resulting concentrated solution at −20 °C, **3** was obtained as yellow crystals (4.95 g, 5.09 mmol, 25.3%). ^{1}H NMR (395.75 MHz, C_6D_6): δ 16.52 (s, 1H, Cp-H), 10.47 (s, 1H × 2, Cp-H), 10.43 (d, 2H, Ph-H [ortho]), 8.97 (d, 2H, Ph-H [ortho]), 7.88 (t, 2H, Ph-H [meta]), 7.55 (t, 1H, Ph-H [para]), 7.10 (t, 2H, Ph-H [meta]), 6.93 (t, 1H, Ph-H [para]), 4.74 (s, 8H, THF-α), 4.62 (s, 1H, Cp-H), 2.03 (s, 8H, THF-β), 1.33 (s, 9H, Me_3Si), −0.65 (s, 9H, Me_3Si), −0.79 (s, 9H, Me_3Si), −2.44 (s, 9H, Me_3Si). Anal. Calcd for $C_{42}H_{66}Cl_2LiO_2Si_5Sm$: Sm, 15.48. Found: Sm, 15.37.

$[1,2\text{-}(Me_2Si)(Me_2SiOSiMe_2)](4\text{-}Me_3CC_5H_2)_2SmCl_2Li_2(THF)_2$ (4a). The aforementioned procedure for **3** was carried out with **10** (2.75 g, 6.38 mmol), nBuLi (1.54 M solution in hexane, 9.0 mL, 13.9 mmol), and $SmCl_3$ (1.55 g, 6.04 mmol) in 70 mL of THF. Recrystallization from hexane yielded 1.76 g (2.20 mmol, 34.4%) of **4a** as yellow crystals. ^{1}H NMR (395.75 MHz, C_6D_6): δ 12.92 (s, 2H, Cp-H), 5.92 (s, 2H, Cp-H), 4.51 (s, 8H, THF-α), 3.14 (s, 3H, Me_2Si), 2.86 (s, 3H, Me_2Si), 2.37 (s, 18H, Me_3C), 1.91 (s, 8H, THF-β), 0.73 (s, 6H, $Me_2SiOSiMe_2$), −3.75 (s, 6H, $Me_2SiOSiMe_2$). ^{13}C NMR (99.45 MHz, C_6D_6): δ 146.4 (Cp), 128.6 (Cp), 125.6 (Cp), 116.9 (Cp), 115.7 (Cp), 69.3 (THF-α), 39.6 (Me_3*C*), 29.9 (*Me*$_3$C), 26.0 (THF-β), 23.0 (MeSi), 14.3 (MeSi), 3.0 (MeSi), −3.4 (MeSi). Anal. Calcd for $C_{32}H_{56}Cl_2LiO_3Si_3Sm$: Sm, 18.77. Found: Sm, 18.32.

$[1,2\text{-}(Me_2Si)(Me_2SiOSiMe_2)](4\text{-}Me_3CC_5H_2)SmCH(SiMe_3)_2$ (4b). The aforementioned procedure for **1b** was carried out with **4a** (1.75 g, 2.18 mmol) and $(Me_3Si)_2CHLi$ (0.61 M solution in ether, 4.5 mL, 2.75 mmol) in 60 mL of toluene. Recrystallization from hexane yielded 0.87 g (1.18 mmol, 54.0%) of **4b** as a red microcrystalline solid. ^{1}H NMR (395.75 MHz, C_6D_6): δ 20.38 (s, 1H, Cp-H or SmC*H*($SiMe_3$)$_2$), 13.09 (s, 1H, Cp-H or SmC*H*($SiMe_3$)$_2$), 12.66 (s, 1H, Cp-H or SmC*H*($SiMe_3$)$_2$), 4.06 (s, 1H, Cp-H or SmC*H*($SiMe_3$)$_2$), 3.89 (s, 3H, Me_2Si), 3.24 (s, 1H, Cp-H or SmC*H*($SiMe_3$)$_2$), 2.83 (s, 9H, Me_3C), 2.59 (s, 9H, Me_3C), 1.30 (s, 3H, Me_2Si), 1.26 (s, 3H, Me_2Si), −0.57 (s, 3H, Me_2Si), −2.25 (s, 9H, Me_3Si), −4.36 (s, 3H, Me_2Si), −4.80 (s, 3H, Me_2Si), −6.30 (s, 9H, Me_3Si). ^{13}C NMR (99.45 MHz, C_6D_6): δ 151.8 (Cp), 149.9 (Cp), 129.0 (Cp), 128.5 (Cp), 127.9 (Cp), 127.6 (Cp), 117.0 (Cp), 116.8 (Cp), 116.1 (Cp), 114.3 (Cp), 41.4, 31.4, 29.9, 8.4, 3.3, 3.1, 1.4, −0.7, −2.6, −3.4, −3.7, −6.6. Anal. Calcd for $C_{31}H_{59}OSi_5Sm$: Sm, 20.35. Found: Sm, 19.92.

***rac*-$Me_2Si[2,4\text{-}(Me_3Si)_2C_5H_2]_2YCl_2Li(THF)_2$ (5a).** A solution of the ligand **8** (3.0 g, 6.3 mmol) in THF (25 mL) was cooled to 0 °C. nBuLi (1.60 M solution in hexane, 8.2 mL, 13.1 mmol) was added to the solution dropwise, and the mixture was stirred and warmed to 23 °C gradually over 6 h. The resulting solution of the lithium dianion of **8** was added to a suspension of YCl_3 (1.82 g, 9.32 mmol) in THF (30 mL), and the mixture was refluxed for 6 h. After the solvent was removed by evaporation, the residual solid was dried under vacuum. Hexane (80 mL) was added to the solid, and the resulting suspension was stirred for 15 h at 23 °C. The insoluble solid was removed by centrifugation. The solvent was removed by evaporation, and the residual solid was dried under vacuum. Recrystallization of the solid from toluene afforded **5a** as colorless crystals (0.72 g, 0.92 mmol, 15%). ^{1}H NMR (400.14 MHz, C_6D_6): δ 7.27 (s, 2H, Cp-H), 6.98 (s, 2H, Cp-H), 3.55 (s, 8H, THF-α), 1.39 (s, 8H, THF-β), 1.13 (s, 6H, Me_2Si), 0.64 (s, 9H, Me_3Si), 0.50 (s, 9H, Me_3Si). Anal. Calcd for $C_{32}H_{62}Cl_2LiO_2Si_5Y$: Y, 11.31. Found: Y, 11.05.

***rac*-$Me_2Si[2,4\text{-}(Me_3Si)_2C_5H_2]_2YCl_2Li(OEt_2)_3$.** This compound was obtained as colorless crystals by recrystallization of **5a** from ether. ^{1}H NMR (395.75 MHz, C_6D_6): δ 7.29 (s, 2H, Cp-H), 6.93 (s, 2H, Cp-H), 3.55 (q, $^3J_{HH} = 7.0$ Hz, 12H, Et_2O-α), 1.09 (s, 6H, Me_2Si), 1.03 (t, $^3J_{HH} = 7.0$ Hz, 18H, Et_2O-β), 0.59 (s, 9H, Me_3Si), 0.47 (s, 9H, Me_3Si). ^{13}C NMR (99.45 MHz, C_6D_6): δ 138.0 (Cp), 130.4 (Cp), 129.4 (Cp), 128.4 (Cp), 125.9 (Cp), 66.0 (Et_2O-α), 25.3 (Me_2Si), 14.9 (Et_2O-β), 2.4 (Me_3Si), 0.4 (Me_3Si). Anal. Calcd for $C_{36}H_{76}Cl_2LiO_3Si_5Y$: Y, 10.29. Found: Y, 11.05.

***rac*-$Me_2Si[2,4\text{-}(Me_3Si)_2C_5H_2]_2YCH(SiMe_3)_2$ (5b).** The aforementioned procedure for **1b** was carried out with **5a** (0.63 g, 0.80 mmol) and $(Me_3Si)_2CHLi$ (0.54 M solution in ether, 1.9 mL, 1.03 mmol) in 40 mL of toluene. Recrystallization from hexane yielded 0.16 g (0.22 mmol, 28%) of **5b** as colorless crystals. ^{1}H NMR (395.75 MHz, C_6D_6): δ 7.70 (s, 1H, Cp-H), 6.99 (s, 1H, Cp-H), 6.81 (s, 1H, Cp-H), 6.65 (s, 1H, Cp-H), 0.98 (s, 3H, Me_2Si), 0.96 (s, 3H, Me_2Si), 0.46 (s, 9H, Me_3Si), 0.39 (s, 9H, Me_3Si), 0.37 (s, 9H, Me_3Si), 0.33 (s, 9H, Me_3Si), 0.27 (s, 9H, Me_3Si), 0.20 (s, 9H, Me_3Si). The YC*H*($SiMe_3$)$_2$ signal was obscured by the other resonances. ^{13}C NMR (99.45 MHz, C_6D_6): δ 137.1 (Cp), 136.8 (Cp), 133.4 (Cp), 131.8 (Cp), 131.5 (Cp), 131.0 (Cp), 129.9 (Cp), 129.6 (Cp), 129.5 (Cp), 129.0 (Cp), 26.6 (d, $^1J_{Y-C} = 31.9$ Hz, Y-*C*H($SiMe_3$)$_2$), 5.9 (Me_3Si), 2.7 (Me_3Si), 2.6 (Me_3Si), 2.1 (Me_3Si), 0.8 (Me_3Si), 0.7 (Me_3Si), 0.5 (Me_2Si), 0.1 (Me_2Si). Anal. Calcd for $C_{31}H_{65}Si_7Y$: Y, 12.29. Found: Y, 11.54.

$Me_2Si[2,4\text{-}(Me_3Si)_2C_5H_2][3,4\text{-}(Me_3Si)_2C_5H_2]YCl_2Li(THF)_2$ (6a). A solution of the ligand **8** (7.0 g, 14.7 mmol) in THF (40 mL) was cooled to 0 °C. nBuLi (1.60 M solution in hexane, 19.5 mL, 31.2 mmol) was added to the solution dropwise, and the mixture was stirred and warmed to 23 °C gradually over 6 h. The resulting solution of the lithium dianion of **8** was added to a suspension of YCl_3 (2.33 g, 11.9 mmol) in THF (40 mL), and the mixture was refluxed for 6 h. After the solvent was removed by evaporation, the residual solid was dried under vacuum. Ether (40 mL) was added to the solid, and the resulting suspension was stirred for 15 h at

23 °C. The insoluble solid was removed by centrifugation. After a part of the solvent was removed by evaporation, the resulting concentrated solution was cooled to −20 °C. **6a** was obtained as colorless crystals (1.72 g, 2.19 mmol, 18.4%). ^{1}H NMR (400.14 MHz, C_6D_6): δ 6.97 (s, 1H, Cp-H), 6.93 (s, 1H, Cp-H), 6.83 (s, 1H, Cp-H), 6.77 (s, 1H, Cp-H), 3.55 (s, 8H, THF-α), 1.39 (s, 8H, THF-β), 1.00 (s, 3H, Me_2Si), 0.99 (s, 3H, Me_2Si), 0.61 (s, 9H, Me_3Si), 0.58 (s, 9H, Me_3Si), 0.56 (s, 9H, Me_3Si), 0.46 (s, 9H, Me_3Si). Anal. Calcd for $C_{32}H_{62}Cl_2LiO_2Si_5Y$: Y, 11.31. Found: Y, 11.22.

$Me_2Si[2,4-(Me_3Si)_2C_5H_2][3,4-(Me_3Si)_2C_5H_2]YCH(SiMe_3)_2$ (6b). The aforementioned procedure for **1b** was carried out with **6a** (1.67 g, 2.12 mmol) and $(Me_3Si)_2CHLi$ (0.86 M solution in ether, 3.0 mL, 2.58 mmol) in 80 mL of toluene. Recrystallization from hexane yielded 0.80 g (1.11 mmol, 52.3%) of **6b** as colorless crystals. ^{1}H NMR (400.14 MHz, C_6D_6): δ 7.66 (s, 1H, Cp-H), 6.61 (s, 1H, Cp-H), 6.56 (s, 1H, Cp-H), 6.50 (s, 1H, Cp-H), 0.86 (s, 3H, Me_2Si), 0.81 (s, 3H, Me_2Si), 0.47 (s, 9H × 2, Me_3Si), 0.41 (s, 9H, Me_3Si), 0.34 (s, 9H, Me_3Si), 0.23 (s, 9H × 2, Me_3Si). The $YCH(SiMe_3)_2$ signal was obscured by the other resonances. Anal. Calcd for $C_{31}H_{65}Si_7Y$: Y, 12.29. Found: Y, 12.04.

$(Me_2Si)(Me_2SiOSiMe_2)(Me_3SiC_5H_3)_2$ (11). A solution of $(Me_3SiC_5H_4)_2SiMe_2$ (22.7 g, 68.5 mmol) in THF (300 mL) was placed in a round-bottomed flask equipped with a condenser and was cooled to 0 °C. nBuLi (1.52 M, 95.0 mL, 144 mmol) was added dropwise to the solution, and the mixture was stirred and warmed to 23 °C over 3 h. $ClMe_2SiOSiMe_2Cl$ (15.0 mL, 76.7 mmol) was added, and the mixture was refluxed for 24 h. The complete disappearance of $(Me_3C_5H_4)_2SiMe_2$ was confirmed by GC analysis. The mixture was poured into 300 mL of $NaHCO_3$ saturated aqueous solution. After extractive workup with hexane and water, bulb-to-bulb distillation of the resulting liquid (200 °C/0.1 mmHg) afforded **11** in 89.9% yield (28.5 g, 61.6 mmol) as a yellow oil. The ^{1}H NMR spectrum of **11** suggested that the compound was a mixture of isomers with respect to the positions of double bonds and substituents on the Cp rings.

$[1,2-(Me_2Si)(Me_2SiOSiMe_2)](4-Me_3SiC_5H_2)YCl(THF)$ (7a). The aforementioned procedure for **1b** was carried out with **11** (4.3 g, 9.3 mmol), nBuLi (1.62 M solution in hexane, 12.0 mL, 19.4 mmol), and YCl_3 (2.40 g, 12.3 mmol) in 50 mL of THF. Recrystallization from hexane yielded 1.38 g (2.10 mmol, 22.6%) of **7a** as colorless crystals. The ^{1}H NMR spectrum of this compound indicated the presence of two kinds of isomers in almost equal amounts in the C_6D_6 solution at 23 °C. ^{1}H NMR (395.75 MHz, C_6D_6): δ 7.25 (s, 2H, Cp-H), 6.76 (s, 2H, Cp-H), 6.70 (s, 2H × 2, Cp-H), 3.53 (s, 8H, THF-α), 1.37 (s, 8H, THF-β), 1.25 (s, 6H, $Me_2SiOSiMe_2$), 1.15 (s, 3H, Me_2Si), 0.93 (s, 3H, Me_2Si), 0.85 (s, 6H, $Me_2SiOSiMe_2$), 0.77 (s, 3H, Me_2Si), 0.55 (s, 6H, $Me_2SiOSiMe_2$), 0.51 (s, 18H, Me_3Si), 0.49 (s, 18H, Me_3Si), 0.34 (s, 3H, Me_2Si), 0.30 (s, 6H, $Me_2SiOSiMe_2$). Anal. Calcd for $C_{26}H_{48}ClO_2Si_5Y$: Y, 13.52. Found: Y, 13.36.

$[1,2-(Me_2Si)(Me_2SiOSiMe_2)](4-Me_3SiC_5H_2)YCH(SiMe_3)_2$ (7b). The aforementioned procedure for **1b** was carried out with **7a** (3.60 g, 5.48 mmol) and $(Me_3Si)_2CHLi$ (0.75 M solution in ether, 9.0 mL, 6.8 mmol) in 60 mL of toluene. Recrystallization from hexane yielded 1.74 g (2.46 mmol, 44.9%) of **7b** as colorless crystals. ^{1}H NMR (395.75 MHz, C_6D_6): δ 7.53 (s, 1H, Cp-H), 7.33 (s, 1H, Cp-H), 6.33 (s, 1H, Cp-H), 6.31 (s, 1H, Cp-H), 1.09 (s, 3H, MeSi), 0.67 (s, 3H, MeSi), 0.66 (d, 1H, $^2J_{Y-H} = 2.53$ Hz, Y-CH($SiMe_3)_2$), 0.59 (s, 3H, MeSi), 0.56 (s, 3H, MeSi), 0.42 (s, 3H, MeSi), 0.40 (s, 3H, MeSi), 0.38 (s, 9H, Me_3Si), 0.30 (s, 9H × 2, Me_3Si), 0.23 (s, 9H, Me_3Si). ^{13}C NMR (99.45 MHz, C_6D_6): δ 138.2 (Cp), 136.7 (Cp), 132.9 (Cp), 132.0 (Cp), 130.9 (Cp), 129.8 (Cp), 129.5 (Cp), 129.0 (Cp), 128.8 (Cp), 128.6 (Cp), 29.1 (d, $^1J_{Y-C} = 32.8$ Hz, Y-CH($SiMe_3)_2$), 5.8 (MeSi), 4.1 (MeSi), 4.0 (MeSi), 2.0 (MeSi), 1.6 (MeSi), 1.3 (MeSi), 0.8 (MeSi), 0.5 (MeSi), 0.4 (MeSi), −3.9 (MeSi). Anal. Calcd for $C_{29}H_{59}OSi_7Y$: Y, 12.53. Found: Y, 12.48.

Typical Procedure for Ethylene Polymerization. A solution of an initiator (0.02 mmol) in 20 mL of toluene was exposed to 1 atm of ethylene. The reaction mixture was stirred for fixed times defined in Table 4 at 23 °C. The polymerization was stopped by the addition of methanol. The resulting polyethylene was washed with methanol twice and dried in vacuo.

Typical Procedure for 1-Olefin Polymerization. To a toluene solution (3 mL) of an initiator (0.02 mmol) was added 2 mL of a monomer at 23 °C. The reaction mixture was stirred for each period defined in Table 5 at 23 °C. The polymerization was stopped by the addition of methanol. The resulting polyethylene was washed with methanol twice and dried in vacuo.

Acknowledgment. This work was supported by a Grant-in-aid for Scientific Research on Priority Areas (No. 283, "Innovative Synthetic Reactions") from the Ministry of Education, Science, and Culture Japan.

Supporting Information Available: Tables of crystallographic data and data collection parameters, atom coordinates, anisotropic displacement parameters, equivalent isotropic displacement parameters, bond distances, bond angles, and hydrogen coordinates for complexes **1a**, **2a**, **2b**, **3**, and **7a**. This material is available free of charge via the Internet at http://pubs.acs.org.

OM000226A